

Electronic Supplementary Information (ESI)

Hybrid mesoporous nanorods with deeply grooved lateral faces toward cytosolic drug delivery

Kaiyao Sun^a, Tao Ding^a, Yuxin Xing^a, Dong Mo^a, Jixi Zhang^{*, a} and Jessica M. Rosenholm^{*, b}

^aKey Laboratory of Biorheological Science and Technology, Ministry of Education, College of
Bioengineering, Chongqing University, No. 174 Shazheng Road, Chongqing 400044, China

E-mail: jixizhang@cqu.edu.cn

^bPharmaceutical Sciences Laboratory, Faculty of Science and Engineering, Åbo Akademi University,

Tykistökatu 6A, Turku 20520, Finland. E-mail: jerosenh@abo.fi

Characterizations.

Transmission electron microscopy (TEM) images, STEM images and EDS-HAADF analysis were obtained using a JEM 2010 (JEOL, Japan) instrument with 200 kV acceleration voltages aiming to inquiry the size, morphology and integrity of the nanoparticles. Samples were dried on holey carbon-coated Cu grids.

Scanning electron microscopy (SEM) measurements were used with a JSM-7800F field emission scanning electron microscope.

The hydrodynamic size distributions and zeta potentials of the particles were measured by applying of dynamic light scattering (DLS) techniques by a Zetasizer Nano instrument (Malvern, UK) at 25 °C.

Nitrogen sorption isotherms were measured with a ASAP2010 analyzer (Micromeritics, USA). The specific surface areas were calculated by the Brunauer-Emmett-Teller (BET) method in a linear relative pressure range between 0.05 and 0.25. The pore size distributions were measured the desorption branches of the isotherms by the NLDFT method.

Thermogravimetric analysis (TGA) was conducted with a Q500 instrument (TA Instruments, USA). The materials were tested under an air atmosphere from 30 °C to 900 °C at a heating rate of 10 °C min⁻¹.

The FT-IR spectra were collected over the range of 4000-400 cm⁻¹ on a Spectrum 100 infrared spectrophotometer (PerkinElmer, USA) using the KBr technique.

Raman spectra were obtained by using a dispersive spectrophotometer Jobin-Yvon LabRam HR Evolution with 325 nm light for sample excitation and a CCD detector cooled to -70 °C. The laser power used was between 0.5 and 4 mW.

The degradation experiments in vitro were performed by immersing nanorods in synthetic body fluid (SBF) solution (pH 7.4) at a particle concentration of 0.1 or 0.3 mg mL⁻¹, respectively. At specific time points: (1 h, 6 h, 1 d, 2 d, 4 d, and 7 d), each sample was centrifuged at 10,000 rpm for 10 min and then collected supernatants were employed for silicon content quantification by the inductively coupled plasma atomic emission spectroscopy (ICP-AES).

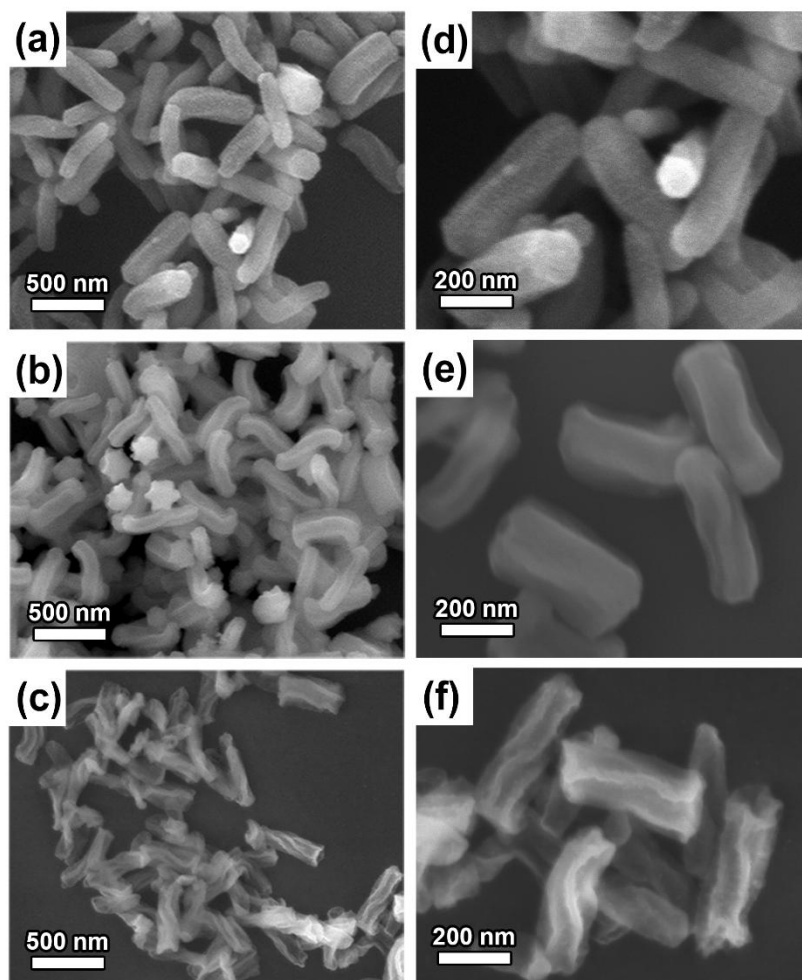


Fig. S1 SEM and magnified SEM observations of twisted nanorods (TNR, a, d) with a hexagon cross-section, TNR-E5 (b, e), and TNR-E20 (c, f).

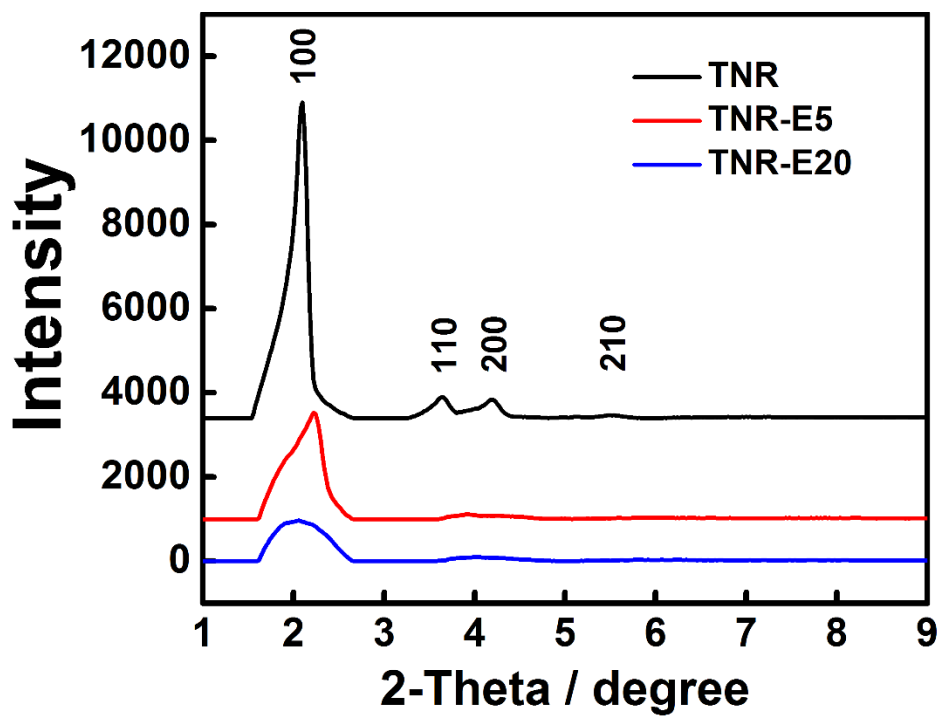


Fig. S2 Powder X-ray diffraction pattern (PXRD) of TNR, TNR-E5, TNR-E20 nanoparticles.

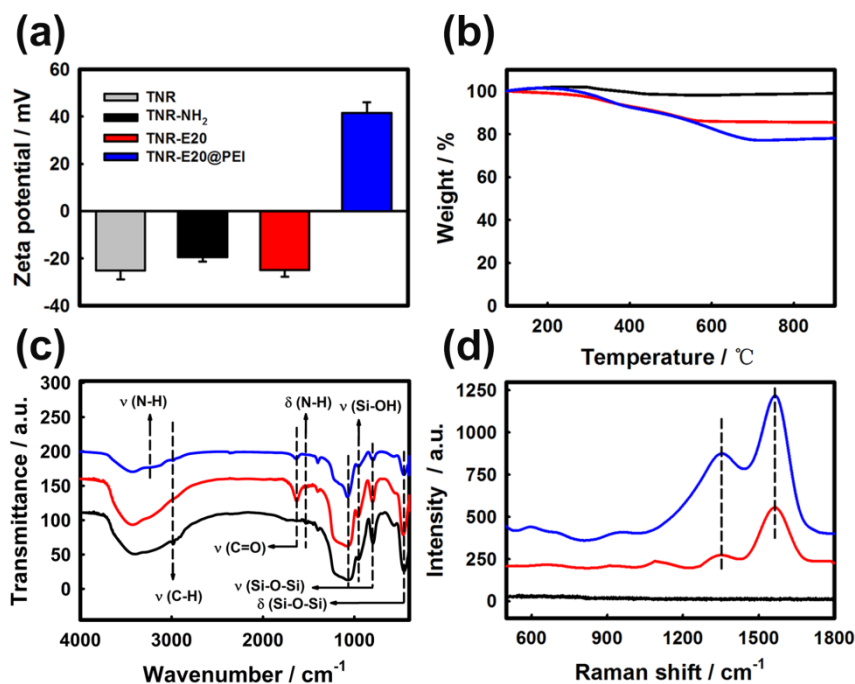


Fig. S3 Zeta potential (a), TGA curves (b), FTIR (c), Raman spectra (d) of the as-prepared amino-modified TNRs (TNR-NH₂), their corresponding products after PDA coating (TNR-E20), and the composite nanoparticles after PEI modification (TNR-E20-PEI).

Zeta potential: The amino-modified TNRs possessed a zeta potential of -19.4 mV which increased by 8.8 mV compared to TNRs. After PDA coating, the surface charge of the particles decreased to -24.8 mV. After PEI modification, the obtained nanoparticles showed a surface charge change from negative to positive (+41.6 mV) owing to the addition of PEI.

Thermogravimetric analysis (TGA): Regarding TNR-E20, an additional weight loss of about 14.7% (more than TNR-NH₂), could be ascribed to the removal of the PDA polymer on the surface of silica. Moreover, TNR-E20-PEI showed maximum weight loss (22%), which was attributed to the degradation of organic components.

Infrared spectroscopy (FTIR): The typical absorption peaks for silica were exhibited at 460 cm⁻¹, 795 cm⁻¹, 954 cm⁻¹, and 1076 cm⁻¹, including the Si-O-Si and Si-OH functional groups.^[1] The strong signal at 1076 cm⁻¹ and the weak signal at 1535 cm⁻¹ were attributed to the asymmetric stretching of Si-O-Si and bending stretching of

NH₂, respectively, confirming the successful functionalization of TNR with amino groups.^[2] After PDA coating on its surface, a broad peak around 3404 cm⁻¹ ascribed to aromatic -NHx and -OH stretching vibrations newly appeared as well as the obvious absorption peaks at 1632 cm⁻¹ (the overlap of C=C resonance vibration in aromatic ring).^[3] Furthermore, TNR-E20-PEI presented broader absorption peaks at around 3404 cm⁻¹ and 3234 cm⁻¹ assigned to vibrations of -NH₂ groups derived from PEI.^[4]

Raman spectroscopy (Raman): The typical peaks of PDA were observed at 1567 cm⁻¹ and 1352 cm⁻¹, which resulted from stretching and deformation of the aromatic rings.^[5-6] As for TNR-E20-PEI, the typical Raman vibrational frequency of PDA was nicely reproduced, evidencing that the structure of the PDA remained intact after modification with PEI.

The above results suggested that the surface of nanorods was successfully functionalized with a large amount of amine group, organic polydopamine and PEI.

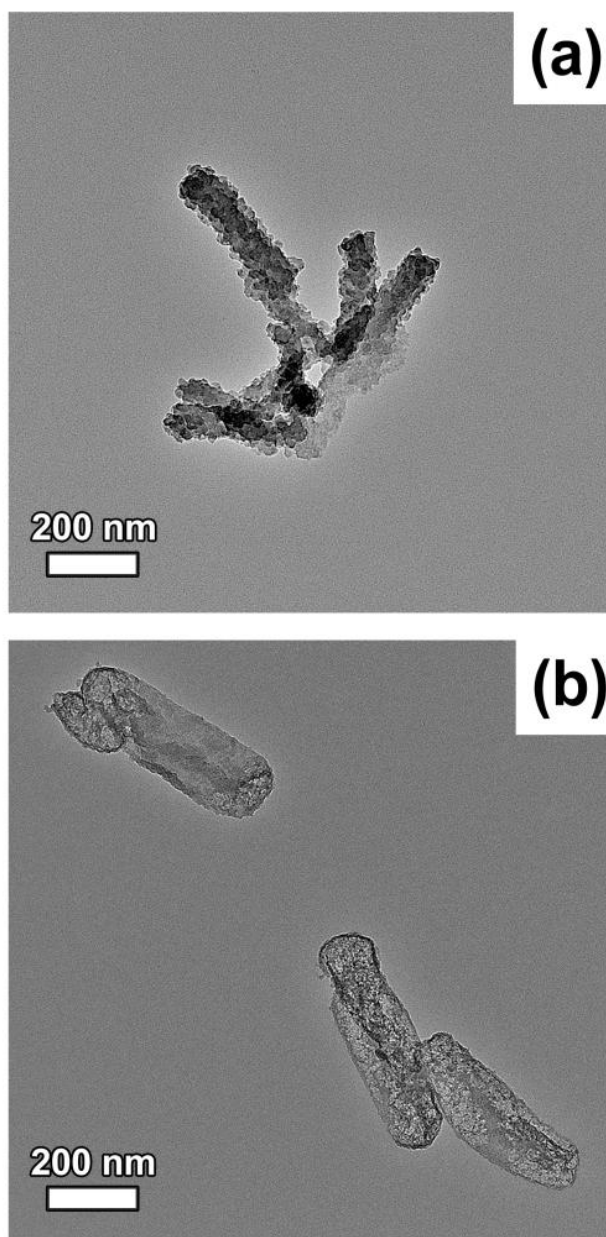


Fig. S4 TEM images of MSNR-E40 (a) and TNR-E40 (b) after PDA coating.

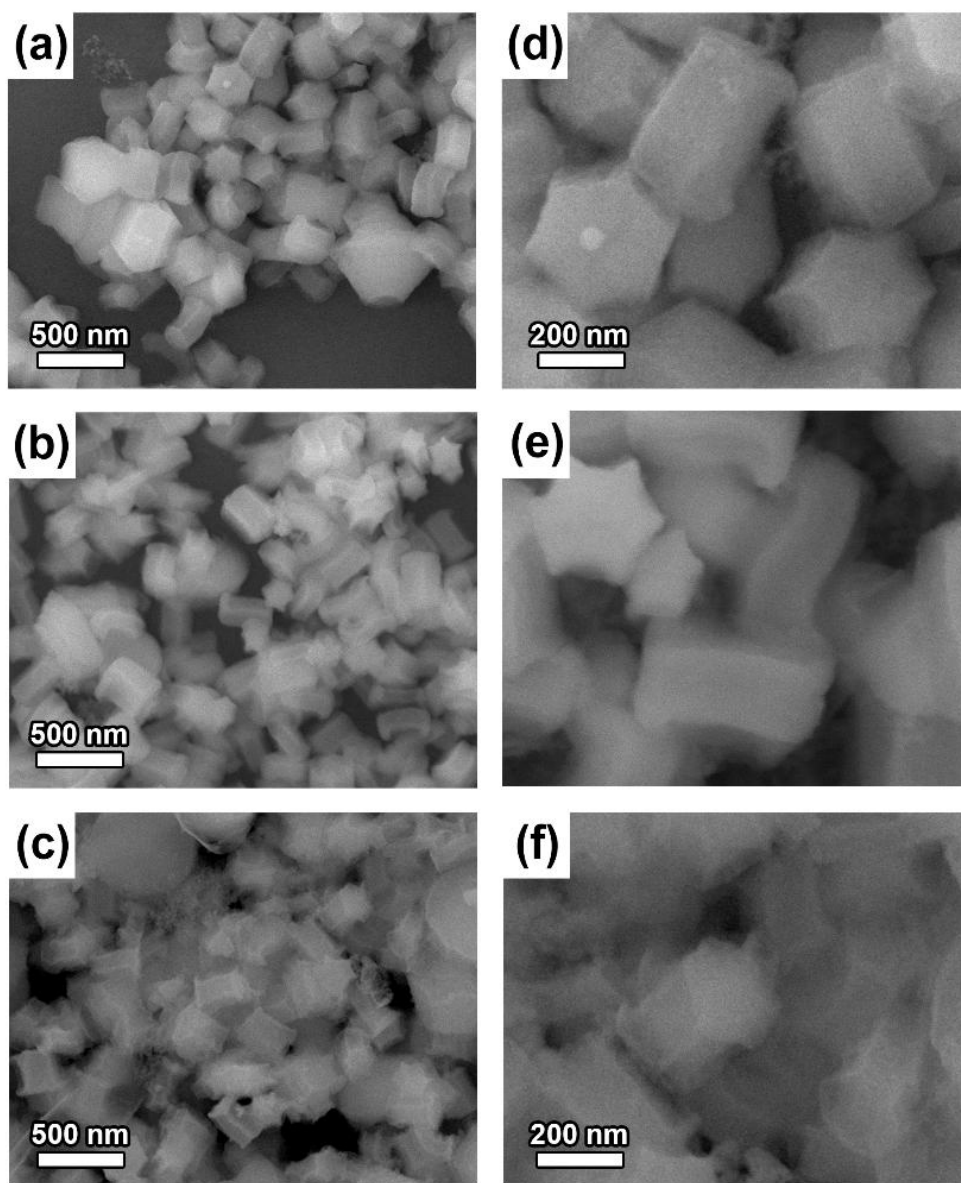


Fig. S5 SEM and magnified SEM observations of short nanorods with a hexagon cross-section (obtained from synthesis at 20 °C, denoted as SNRs, a and d), SNR-E5 (b and c), SNR-E20 (c and d).

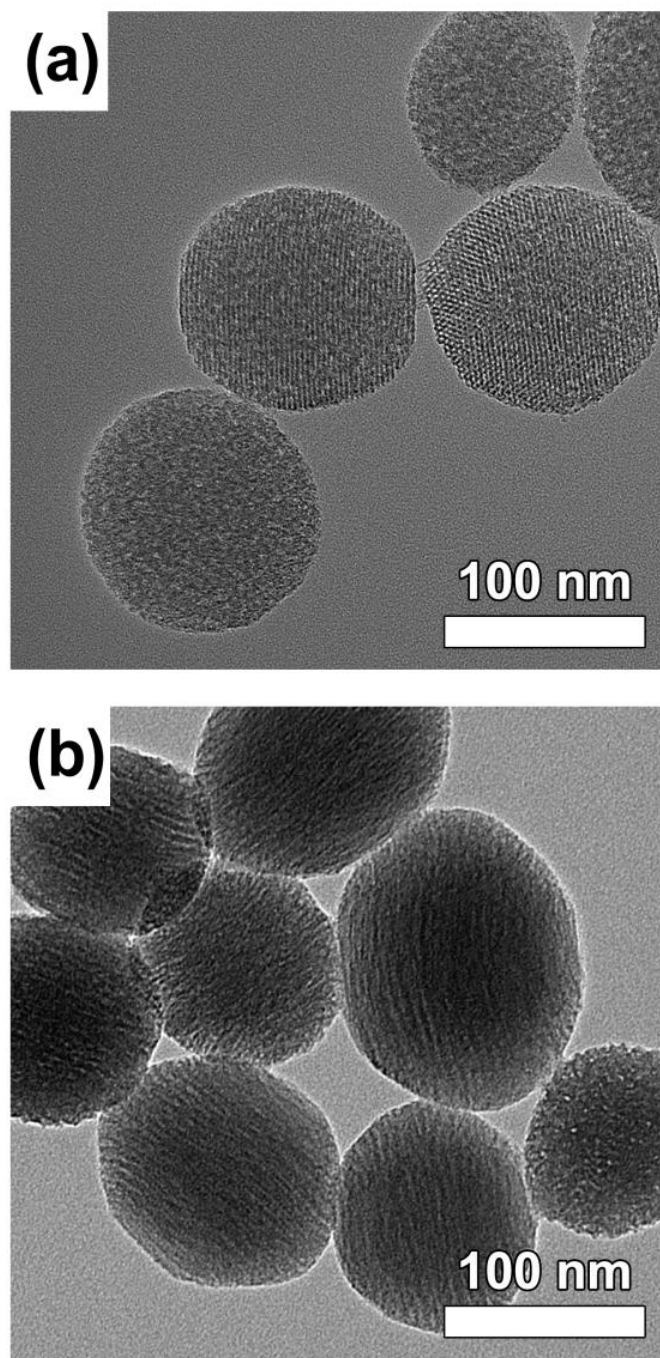


Fig. S6 TEM images of SMSNs (a) and Sphere-E5 (b). The diameter of particles is 100 nm.

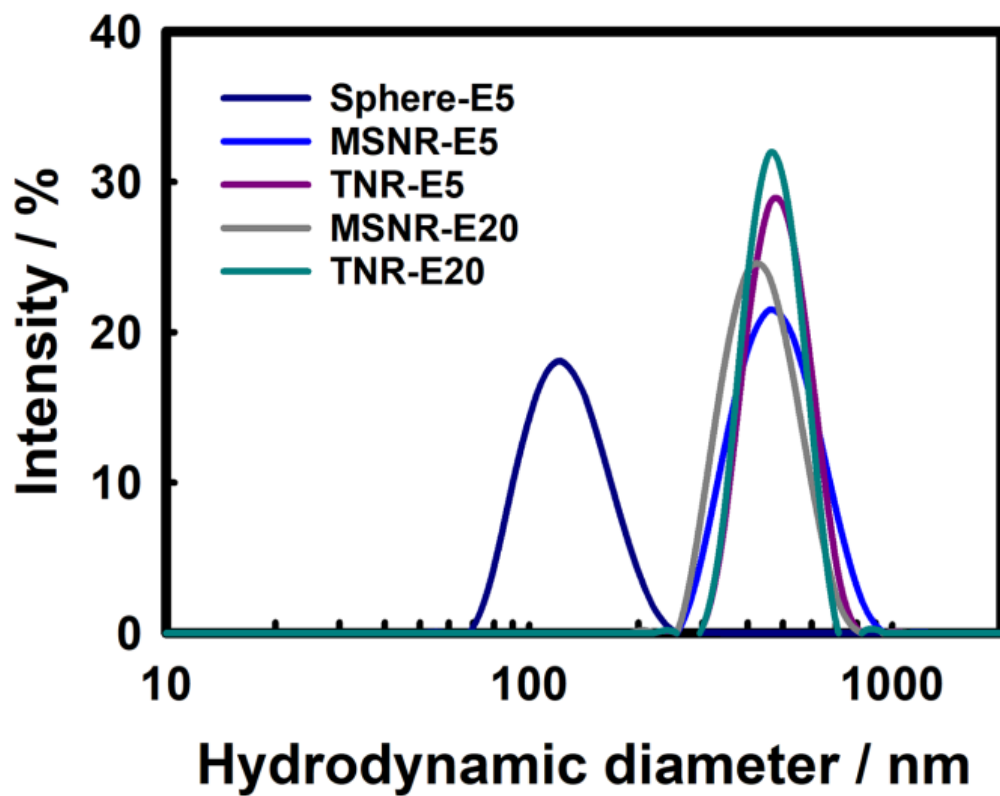


Fig. S7 Hydrodynamic diameter distribution of five types of nanoparticles determined by DLS in HEPES buffer solution.

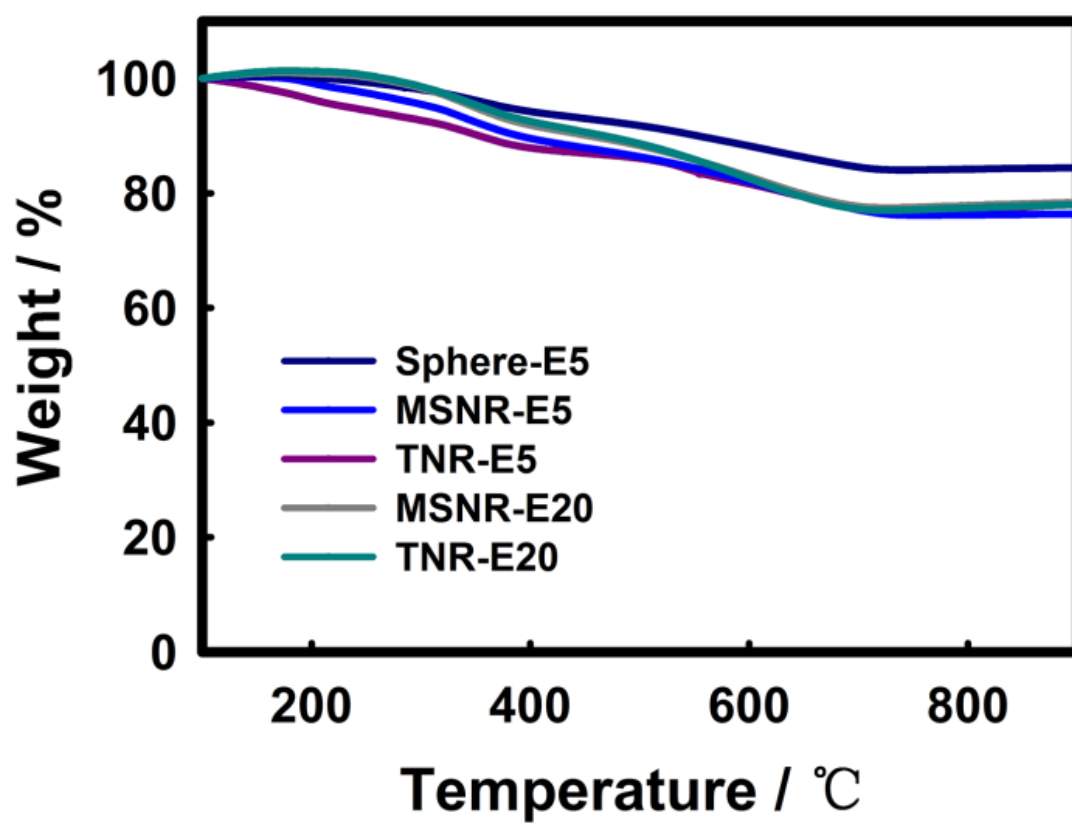


Fig. S8 TGA curves of five types of nanoparticles.

Table S1. Characteristics of five types of nanoparticles.

Sample	Shape	Aspect ratio (length: width)	Hydrodynamic diameter (nm)	Zeta potential (mV)	BET Surface Area (m²g⁻¹)	Pore volume (cm³g⁻¹)
Sphere-E5	Sphere	1	129±12	43.7±1.7	471	0.5
MSNR-E5	long rod	4	474±18	39.1±1.8	753	0.7
TNR-E5	long rod	4	479±24	38.2±1.4	639	0.8
MSNR-E20	long and rough rod	4	454±21	39.9±2.7	631	0.6
TNR-E20	long and rough rod	4	477±7	41.6±4.5	621	0.7

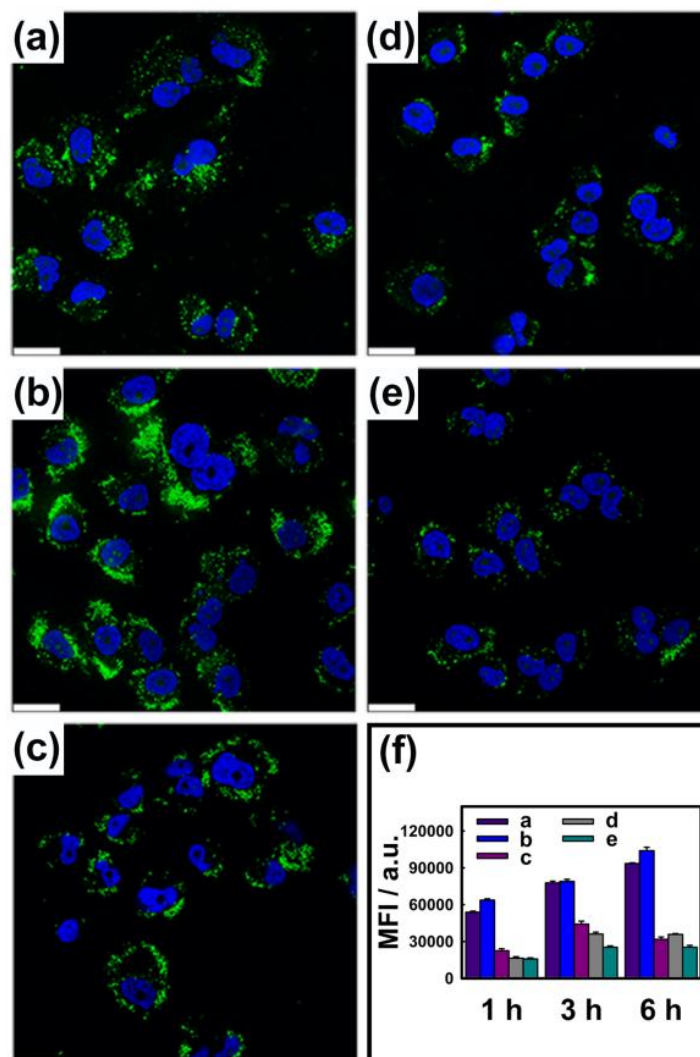


Fig. S9 Confocal microscopy images of MCF-7 cells after 6 h incubation with Sphere-E5 (a), MSNR-E5 (b), TNR-E5 (c), MSNR-E20 (d) and TNR-E20 (e); comparison of the mean fluorescence intensity of five different types of particles incubated with MCF-7 cells for 1 h, 3 h, and 6 h (f). The green fluorescence was from FITC used to modified particles and the blue fluorescence was from Hoechst 33258 used to stain the nuclei. The scale bar represents 25 μm .

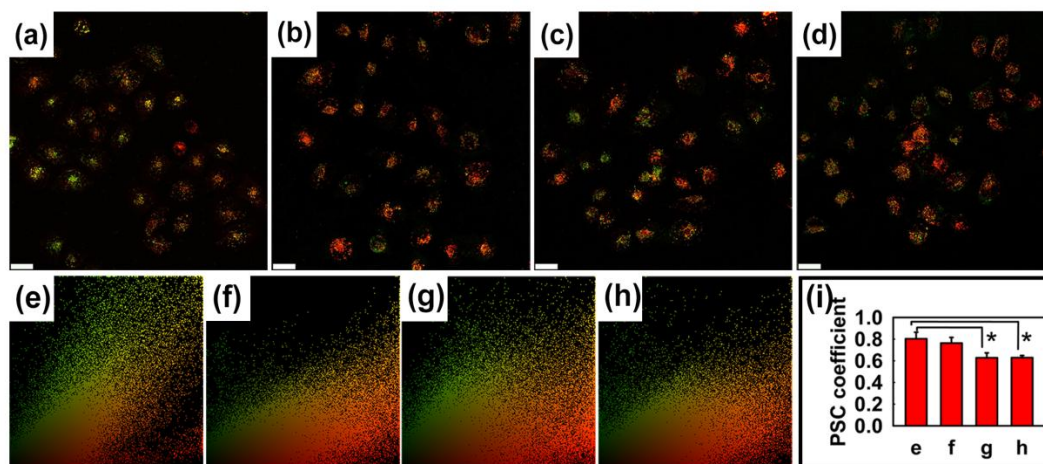


Fig. S10 CLSM images and intensity scatterplot of fluorescence signals of MCF-7 cells incubated with $250 \mu\text{g mL}^{-1}$ of FITC-dextran (a and e) or $100 \mu\text{g mL}^{-1}$ of Sphere-E5 (b and f), TNR-E5 (c and g) or MSNR-E20 (d and h) for 24 h, representing FITC-dextran (green), five kinds of particles (green) and LysoTracker red (red); Bar chart to illustrate the PSC coefficients (i) from (e, f, g and h); The green fluorescence was from FITC dye used to label nanoparticles and the red fluorescence was from LysoTracker red used to stain the lysosome. The scale bar in (a) to (d) represents $25 \mu\text{m}$. (Data are the means \pm SD from three separate experiments. *or ** denotes statistical significance for the comparison of lysosome co-localization numbers between different shaped particles, * $p < 0.05$, ** $p < 0.01$).

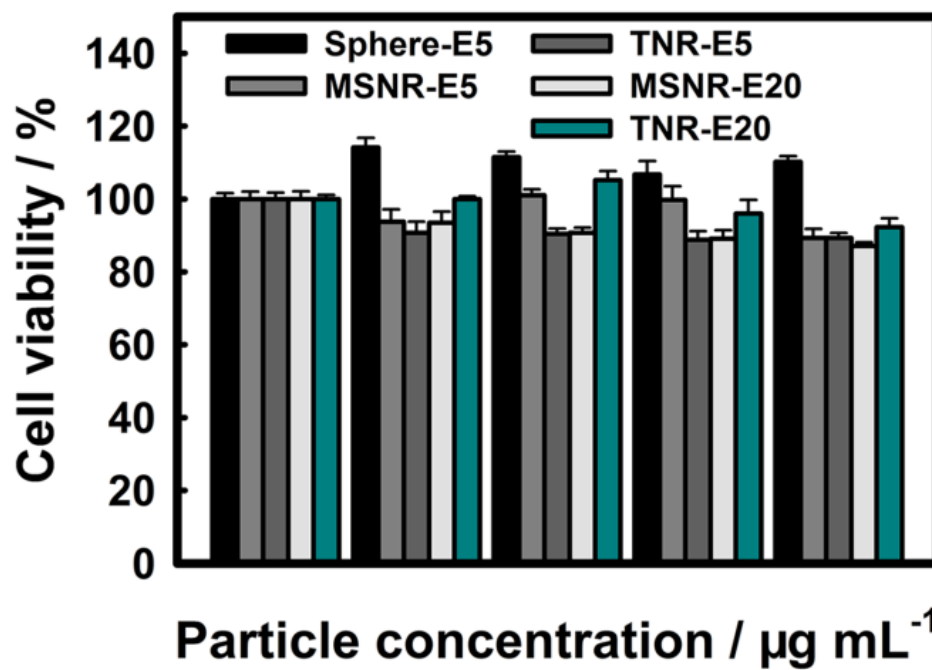


Fig. S11 Quantitative evaluation of the cell viability for MCF-7 cells treated with five types of particles at varying concentrations ranging from $10 \mu\text{g mL}^{-1}$ to $100 \mu\text{g mL}^{-1}$ for 24 h.

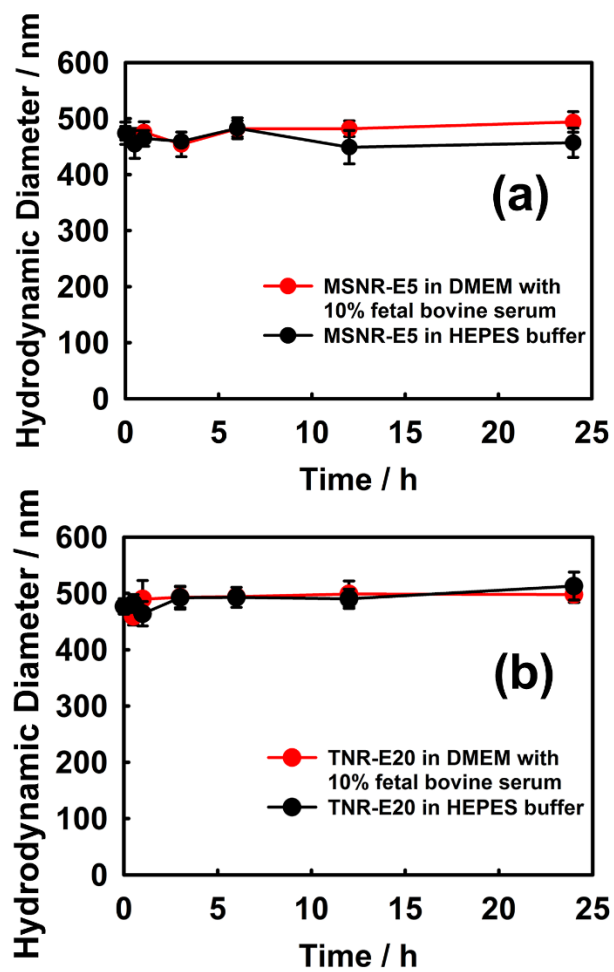


Fig. S12 Stability study of MSNR-E5 (a) and TNR-E20 (b) in Dulbecco's modified Eagle's medium (DMEM, high glucose, Sigma) supplemented with 10% fetal bovine serum (red line) or HEPES (black line) for 24 h by monitoring the average hydrodynamic diameters.

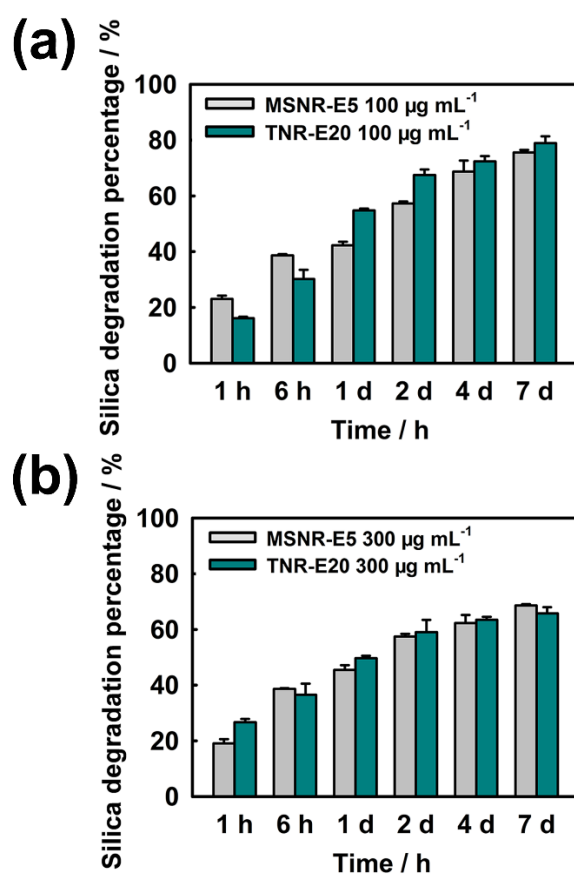


Fig. S13 Silica degradation percentages evolution of MSNR-E5 and TNR-E20 at the different concentrations in SBF solution: 0.1 mg mL⁻¹ (a), 0.3 mg mL⁻¹ (b).

References.

1. X. Zheng, J. Zhang, J. Wang, X. Qi, J. M. Rosenholm and K. Cai, *J. Phys. Chem. C*, 2015, **119**, 24512-24521.
2. G.-M. Bao, L. Wang, H.-Q. Yuan, X.-Y. Wang, T.-X. Mei and M.-R. Qu, *RSC Adv.*, 2016, **6**, 109453-109459.
3. R. Luo, L. Tang, S. Zhong, Z. Yang, J. Wang, Y. Weng, Q. Tu, C. Jiang and N. Huang, *ACS Appl. Mater. Interfaces*, 2013, **5**, 1704-1714.
4. J. Yuan, Z. Zhang, M. Yang, W. Wang, X. Men and W. Liu, *Composites Sci. Technol.*, 2018, **160**, 69-78.
5. H. Guan, L. Wang, J. Zhang, Y. Xing and K. Cai, *Part. Part. Syst. Charact.*, 2018, **35**, 1800011.
6. Y. Ma, X. Zhang, Y. Cheng, X. Chen, Y. Li and A. Zhang, *New J. Chem.*, 2018, **42**, 18102-18108.